Robust Multivariable Flutter Suppression for Benchmark Active Control Technology Wind-Tunnel Model

Martin R. Waszak*
NASA Langley Research Center, Hampton, Virginia 23681-2199

The Benchmark Active Controls Technology project is part of NASA Langley Research Center's Benchmark Models Program for studying transonic aeroelastic phenomena. In January 1996, the Benchmark Active Controls Technology wind-tunnel model was used to successfully demonstrate the application of robust multivariable control design methods (H-∞ and θ-synthesis) to flutter suppression. This paper addresses the design and experimental evaluation of robust multivariable flutter suppression control laws with particular attention paid to the degree to which stability and performance robustness was achieved.

Nomenclature

$F_{(\cdot)}(s)$ = antialiasing and time-delay filters
$G_g(s)$ = gust-model transfer matrix
$G_0(s)$ = nominal-plant transfer matrix
g = gravitational acceleration
M = Mach number
q = dynamic pressure
$W_c(s)$ = control weighting function
$W_p(s)$ = performance weighting function
$W_y(s)$ = output weighting function
$W_0(s)$ = uncertainty weighting function
Δ = uncertainty model
$\bar{\sigma}$ = maximum singular value
$\underline{\sigma}$ = minimum singular value

I. Introduction

ACTIVE control of aeroelastic phenomena, especially in the transonic speed regime, is a key technology for future aircraft design.[1] The Benchmark Active Controls Technology (BACT) project is part of NASA Langley Research Center's Benchmark Models Program[1,2] for studying transonic aeroelastic phenomena. The BACT wind-tunnel model was developed to collect high-quality unsteady aerodynamic data (pressures and loads) near transonic flutter conditions. Accomplishing this objective required the design and implementation of active flutter suppression. Two spoiler-type control effectors were used to investigate the potential for using spoilers to suppress wing flutter. In addition, multiple control surfaces and sensors enabled the investigation of multivariable flutter suppression. An added benefit of multivariable control laws was to provide an opportunity to evaluate the effectiveness of an on-line controller performance evaluation (CPE) tool[3] to assess open- and closed-loop stability robustness of multivariable systems.

The control law designs were performed in two stages. The first stage involved the design and test of single-input/single-output (SISO) controllers to demonstrate and assess the potential for using spoilers to suppress wing flutter. Because similar designs have been successful in the past,[4] this approach also served to reduce the risk of implementing active flutter suppression and thereby increase the probability of achieving the program objectives. The SISO control results also provided a benchmark for evaluating the benefits of multi-input/multi-output (MIMO) control. The second stage involved the design and test of MIMO controllers to demonstrate the potential for enhanced performance and robustness afforded by the robust multivariable design methods.

The design strategy involved using a single fixed control law to suppress flutter over the anticipated range of wind-tunnel operating conditions (rather than using a scheduled control law, for example). This served to simplify the controller implementation and data analysis and is representative of how flutter suppression could be effectively implemented on an actual aircraft. This same strategy was applied to both the SISO and MIMO control law designs.

Before the design and analysis of the control laws is discussed, a short description of the wind-tunnel model and the mathematical model used for the control design is presented. The design objectives are then discussed followed by discussions of the SISO and MIMO design efforts. Finally, analysis and wind-tunnel test results will be presented.

II. BACT Wind-Tunnel Model

A. Physical Model

The BACT system consists of a rigid wing section and a flexible mounting system[5] as shown in the photograph in Fig. 1. The rigid, rectangular wing has an NACA 0012 airfoil section. It is equipped with a trailing-edge control surface and upper- and lower-surface spoilers, which are controlled independently by hydraulic actuators. The lower spoiler (not visible) is identical in size, shape, and relative location to the upper spoiler. The wing section is instrumented with pressure transducers, accelerometers, control surface position sensors, and hydraulic pressure transducers. The accelerometers are the primary sensors for feedback control and are located at each corner of the wing.

The wing is mounted to a device called the pitch-and-plunge apparatus (or PAPA), which is designed to permit motion in principally two modes—rotation (or pitch) and vertical translation (or plunge). The PAPA is instrumented with strain gauges to measure normal force and pitching moment and is mounted to a turntable that can be rotated to control the wing angle of attack. During operation, the mounting system is isolated from the wing section by a splitter plate and from the airflow by a faring that is secured to the splitter plate and the wall of the test section.

The combination of the BACT wing section and PAPA mount will be referred to as the BACT system. The BACT system was precisely tuned to flutter within the operating range of the NASA Langley Transonic Dynamics Tunnel[6] in which the system was tested. The range of Mach number and dynamic pressure over which flutter testing was performed permits the study of transonic aeroelastic phenomena. The transonic flutter dip for the BACT system occurs for a range of Mach numbers from about 0.70 to 0.85. For a Mach number of about 0.77, the flutter frequency is approximately 4 Hz (25.1 rad/s), and the flutter dynamic pressure is approximately 148 psf. More detailed descriptions of both the BACT wing section and the PAPA mounting system can be found in Refs. 5 and 7.

*Senior Research Engineer, Dynamics and Control Branch. Senior Member AIAA.
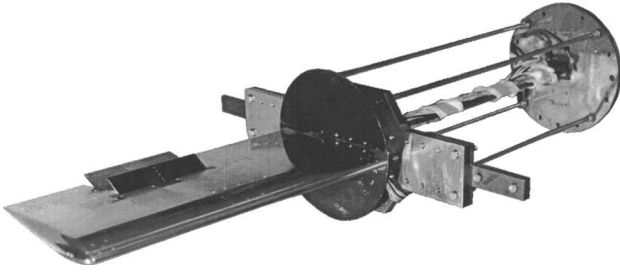
Fig. 1   Photograph of BACT wing section and flexible mount.

The feedback control system for the BACT was implemented with a digital computer running at 200 samples per second. First order 25-Hz antialiasing filters were provided as part of the wind-tunnel model system for each accelerometer channel. These filters provided an acceptable level of attenuation at frequencies beyond the 100-Hz folding frequency and had the virtue of introducing relatively little phase lag at frequencies near flutter. The digital controller implementation also generated a 0.005-s computational delay that introduced additional lag into the system.

B.   Mathematical Model

A mathematical model of the BACT system was developed from first principles expressly for application to control system design. The emphasis of the modeling process was to accurately represent the dynamic characteristics of the BACT system in the frequency range near flutter and over a wide range of wind-tunnel operating conditions. The development of the mathematical model is presented in Ref. 8. The model includes the structural dynamics, aerodynamics, and actuator dynamics. In addition, a simple model of the wind-tunnel turbulence was developed from experimental data. The complete state-space design model is parameterized by dynamic pressure and has 10 states: the four states associated with the pitch-and-plunge degrees of freedom, two states each for the trailing-edge surface and upper spoiler actuators, and two states associated with the wind-tunnel turbulence. A third-order Pade approximation filter was used to model the effect of time delay in the controller. The units on the control inputs are in degrees, and the units on the acceleration outputs are in g. Stability and control derivatives were only available for a single Mach number of 0.77 but produce dynamic response characteristics that are representative of the Mach-number range over which the wind-tunnel tests were performed.

III.   Flutter Suppression Design

The active flutter suppression design was performed in two phases: a SISO design phase and a MIMO design phase. This paper will focus on the MIMO designs; however, the SISO designs will be reviewed to provide a basis for comparison.

There were essentially four main design objectives for all of the flutter suppression control designs: 1) maintain stability over the entire range of operation (robust stability), 2) significantly reduce pitch-and-plunge accelerations at all operating conditions (robust performance), 3) minimize required control activity (both deflections and rates), and 4) use a single, low-order controller to simplify implementation and reduce risk.

A.   SISO Designs

Two SISO control laws were designed and implemented: one controller used the trailing-edge flap and the other used the upper spoiler for control. The trailing-edge flap control law design is described in Ref. 9. The design essentially sought to maximize robustness over the range of dynamic pressures using a single, fixed dynamic compensator element and with a fixed blending of the inboard leading- and trailing-edge accelerometers signals (LEI and TEI, respectively) for feedback. A plot of the control law frequency response is shown in Fig. 2a. The only difference in phase between the two accelerometer channels is caused by the sign on the blending ratio.

The upper spoiler SISO controller was designed using classical design concepts similar to those used in Ref. 4. The difference of the two inboard accelerometer signals is used to produce the controller input. In addition, a controller was sought for which phase and
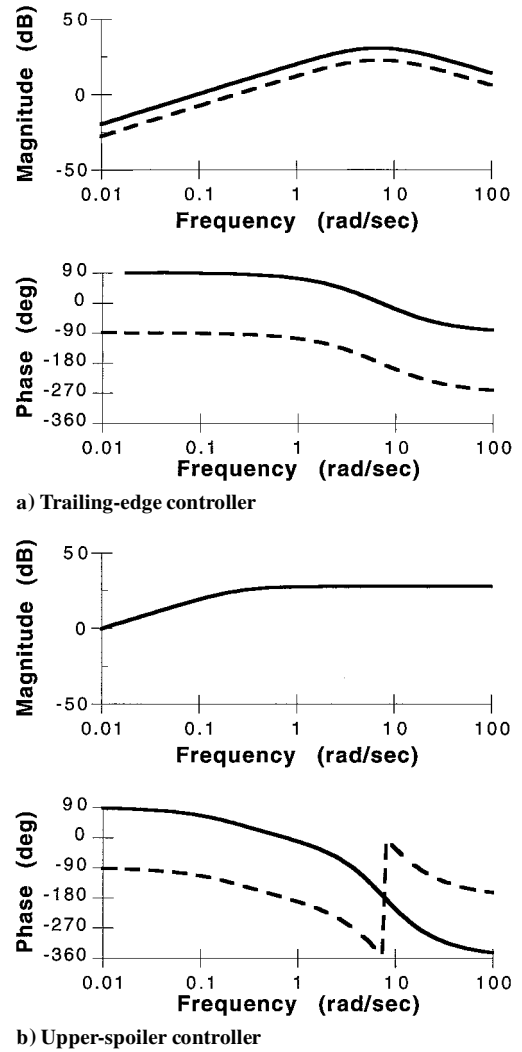

a) Trailing-edge controller

b) Upper-spoiler controller

Fig. 2   SISO controllers: ——, TEI accelerometer, and - - - -, LEI accelerometer.

gain could be altered independently to introduce specific gain and phase variations to assess the ability of the CPE tool[3] to effectively determine stability margins from experimental response data. This was accomplished by making the controller all-pass. A first-order high-pass "washout" filter was added to make the controller insensitive to biases and low frequency disturbances (e.g., amplifier drift in the accelerometer signals). Additional attenuation at frequencies far above the flutter frequency, was provided by the antialiasing filters (and actuator dynamics). A plot of the controller frequency response is shown in Fig. 2b. The high-frequency roll off provided by the antialiasing is not shown. A state-space representation of the upper-spoiler control law is shown in the following equation:

$$\dot{x} = \begin{bmatrix} -0.25 & 0 & 0 \\ -0.25 & -13.33 & -59.26 \\ 0 & 1 & 0 \end{bmatrix} x + \begin{bmatrix} 0.9696 & -0.9696 \\ 0.9696 & -0.9696 \\ 0 & 0 \end{bmatrix} \begin{Bmatrix} \ddot{z}_{TEI} \\ \ddot{z}_{LEI} \end{Bmatrix}$$

$$\delta_{US} = \begin{bmatrix} -6.25 & -666.67 & 0 \end{bmatrix} x + \begin{bmatrix} 24.24 & -24.24 \end{bmatrix} \begin{Bmatrix} \ddot{z}_{TEI} \\ \ddot{z}_{LEI} \end{Bmatrix}$$

B.   MIMO Designs

The MIMO designs using the trailing-edge and upper-spoiler controls and the two inboard accelerometers were developed using H-∞ and μ-synthesis design methods.[10,11] These methods produce multivariable control laws that provide stability robustness to modeled uncertainties in the former case and stability and performance robustness to modeled uncertainties in the latter case and are very amenable to flutter suppression applications, where robust stability subject to limited control activity is a key requirement. The multivariable control law designs were performed after the SISO designs
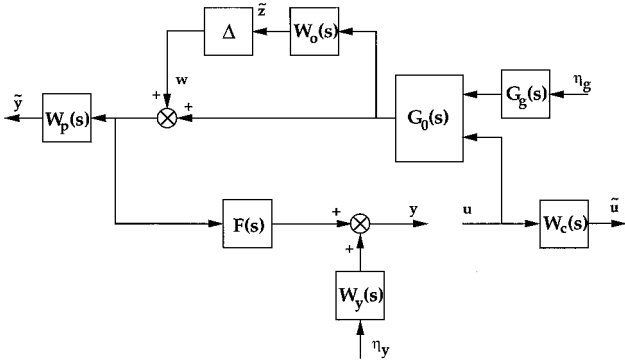
Fig. 3   P-Δ model for the BACT system.

Fig. 4   Averaged design model frequency response compared to ensemble set (——, average, and - - - -, ensemble: $M = 0.77, q = 155, 165, 175, 185,$ and 195 psf).

Fig. 5   Uncertainty model frequency response compared to ensemble set (——, uncertainty, and - - - -, ensemble: $M = 0.77, q = 155, 165, 175, 185,$ and 195 psf).

were implemented and tested on the BACT wind-tunnel model. The MIMO designs benefited greatly from the lessons learned during the SISO design and test phase. In addition, the results of the SISO tests were used to assist in the development of the design specifications for the MIMO control laws.

P-Δ Model Structure

The application of the H-∞ and μ-synthesis methods require a special model structure that isolates key input and output response variables associated with the various performance and robustness requirements. The P-Δ model structure shown in Fig. 3 was developed to combine the basic plant dynamics with various weighting functions associated with the required levels of performance, control power, and uncertainty in the plant model. Each of the elements in this structure will be discussed briefly.

Plant model.   The plant model is associated with three of the block elements in Fig. 3: the nominal BACT system including actuator dynamics $G_0(s)$, the turbulence model $G_g(s)$, and the antialiasing filters and controller time-delay approximation $F(s)$. The turbulence model $G_g(s)$ and the filters $F(s)$ are state-space realizations of the models described in Ref. 8.

The nominal BACT system model was developed to address the objective to design a single control law that would maintain stability over the entire range of anticipated wind-tunnel operating conditions (Mach and dynamic pressure variations). A model-averaging approach[12] was used. This approach generates a single model that passes through the "middle" of the frequency responses of a given ensemble of models and provides a means by which an uncertainty model can be formulated. The model averaging approach was applied to an ensemble of plant models corresponding to the range of dynamic pressures associated with unstable conditions so as not to change the number of right-half-plane eigenvalues of the perturbed plant relative to the nominal plant.

A key step in the model-averaging approach is order reduction because the averaging process results in potentially very high-order systems—the order of the design model multiplied by the number of models in the ensemble. The approach used here differs from that used in Ref. 12 in that, even though internally balanced reduction was used in both cases, frequency weighting[13] was required to ensure that the frequency response of the averaged model had the proper slope at low frequencies. In addition, the reduced-order average model was chosen to exhibit two aeroelastic modes like the actual BACT system. As a result, the model that resulted only approximates the full-order average model. Figure 4 shows a representative frequency response plot (trailing-edge acceleration as a result of trailing-edge control) for the reduced-order average model and the ensemble upon which it is based. The other input-output pairs are similar.

Uncertainty representation.   An unstructured output multiplicative uncertainty model was obtained from the average model and the ensemble. The uncertainty model represents an upper bound on the maximum singular values of the difference between the average model and the ensemble. A simple fourth-order transfer function was selected so that $|W_0(s)| \geq \max_i \{\bar{\sigma}[G_i(s) -$
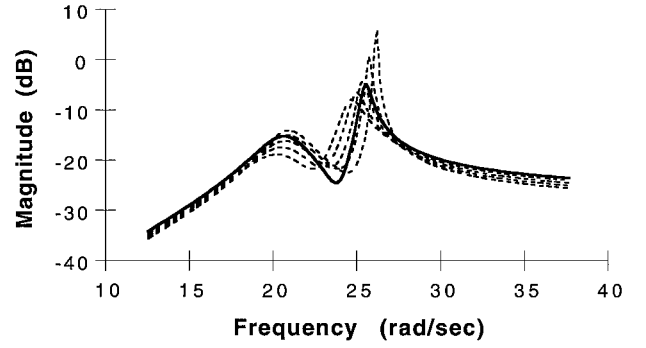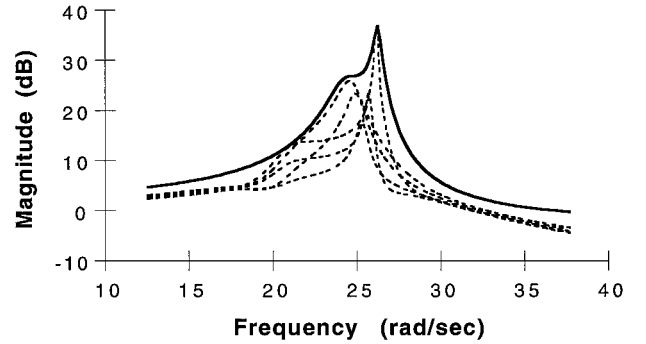
$G_0(s)] \underline{\sigma}[G_0(s)]\} \geq \bar{\sigma}(\Delta)$, where i is the number of models in the ensemble. Figure 5 depicts the frequency response magnitude for the uncertainty model.

Weighting functions.   The performance, control, and output weighting functions, $W_p(s)$, $W_c(s)$, and $W_y(s)$, respectively, were chosen to achieve similar levels of performance and control activity as were achieved by the SISO controllers. Two sets of performance and control weights were considered: a simple set chosen primarily to achieve desired acceleration response and control activity and a more complex set chosen to shape more precisely the frequencies over which the controller would operate.

The simple weights set the maximum acceleration level and control deflections over a range of frequencies from zero to beyond the folding frequency. Data from the SISO controller experiments indicated that attenuation to rms levels of 0.03 g was achievable with rms control activity around 0.3 deg. The performance weight was chosen so that the peak acceleration level for either pitch or plunge would not exceed 0.1 g. The control weight was chosen so that peak control deflections of the trailing-edge flap and upper spoiler would not exceed 1.0 deg.

The complex weights put more emphasis on keeping control activity limited to the frequencies near flutter by penalizing acceleration and control activity in a narrower frequency band (roughly 1–100 rad/s). The performance weight was again chosen to keep accelerations below about 0.1 g. The control weight in this case was less stringent and limited peak deflections to approximately 3.0 deg. Figure 6 shows the two sets of performance and control weights used in the MIMO designs.

The output weighting function $W_y(s)$ is required for the H-∞ algorithms to work. The accelerometers were believed to be quite accurate, and so the weights were chosen to be a small constant value 1e-04. (In retrospect, it would have been desirable to select this weight to reflect large accelerometer errors at low frequencies to generate washout in the controller rather than adding it after the fact as was done.)
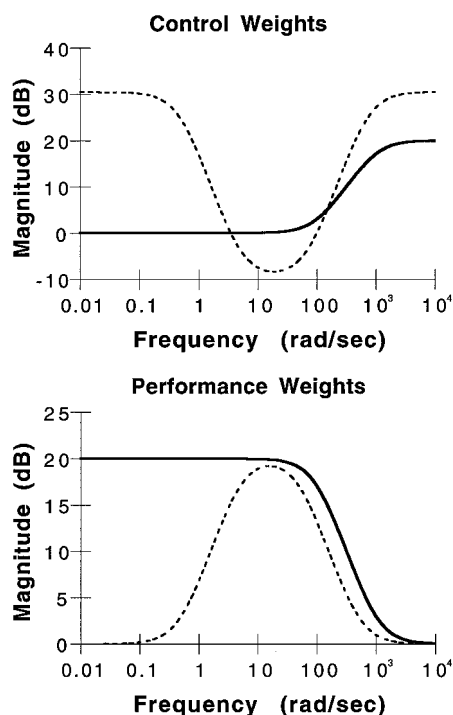
Fig. 6 Control and performance weighting functions for H-∞ and θ-synthesis applications (——, simple weights, and - - - -, complex weights).

H-∞ Designs

The H-∞ control law designs were computed using the μ-Analysis and Synthesis Toolbox[10] for use with MATLAB®. Two controllers were designed with the H-∞ approach using the plant model, the two sets of performance and control weights, and output weight. However, the design algorithm was unable to obtain a control law when the uncertainty model derived from the average plant model was used. As a result, a simple unit-ball uncertainty $W_0(s) = 1$ was used instead and resulted in acceptable designs.

Once the control laws were obtained, washout filters (identical to those used for the SISO spoiler control law) were added to make the controller insensitive to biases and low-frequency disturbances. The added washout filters were required even for the design based on the complex weights because sufficient attenuation (especially near zero frequency) could not be achieved. This was particularly important because the amplifiers associated with the accelerometers used for feedback exhibited significant bias and low-frequency drift.

Control law H-∞ #1, based on the simple weights, was 29th order. Control law H-∞ #2, based on the complex weights, was 37th order. The addition of two first-order washout filters further increased the controller order by two. The largest control law that could be accomodated by the digital controller was 26th order, so both of these control laws were too large to fit within the digital controller. As a result, controller order reduction was employed to reduce the order. Internally balanced reduction[13] was used to reduce the model order without sacrificing frequency response accuracy near flutter (10–100 rad/s). The final order for control laws H-∞ #1 and H-∞ #2 was 7 and 12, respectively. Figures 7 and 8 depict the frequency responses of the two reduced-order control laws that were tested in the wind tunnel.

μ-Synthesis Designs

The μ-synthesis control law designs were also computed using the μ-Analysis and Synthesis Toolbox.[10] Three controllers were designed with the μ-synthesis approach using the same plant model and performance, control, output, and unit-ball uncertainty weights used for the H-∞ designs.

The solution of the μ-synthesis problem involves an iterative process, D-K iteration.[10] This iterative process does not, however, converge to a unique controller. The designer must choose the number of iterations needed, whether or not the desired level of robustness (i.e., $\mu \leq 1$) can be achieved and if the robustness of the current iter-
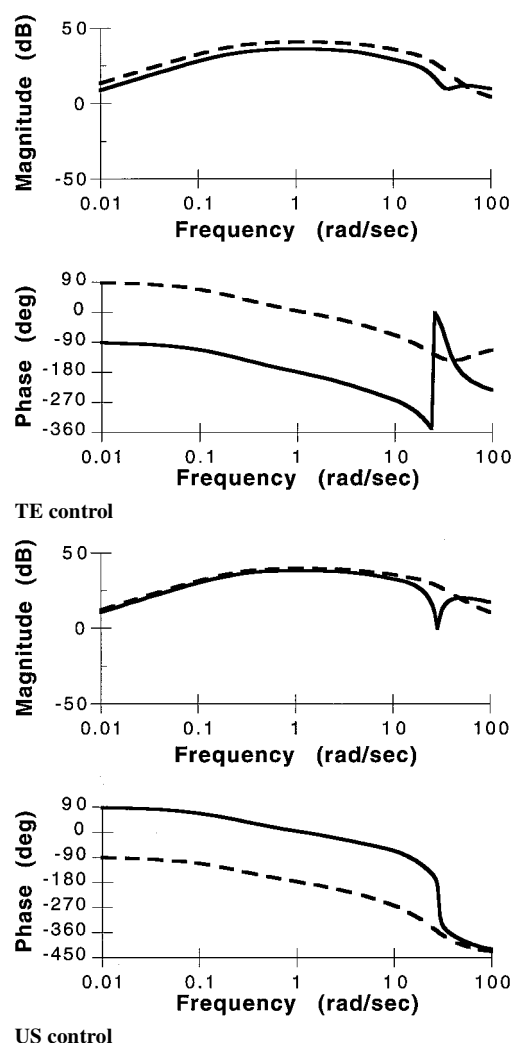

TE control

US control

Fig. 7 H-∞ #1 frequency response: ——, TEI accelerometer, and - - - -, LEI accelerometer.

ate is acceptable. Sensitivity of the D-K iteration procedure to initial conditions and parameter selections (e.g., γ and D-scale approximations) resulted in difficulty arriving at acceptable μ-synthesis controllers, but the final full-order μ-synthesis control laws did have structured singular values that were all near unity.

Control laws μ #1 and μ #2, based on the simple weights, were 31st and 29th order, respectively. These designs differ because of the choices for γ and D-scale approximations. Control law μ #3, based on the complex weights, was 35th order. Once the control laws were obtained, washout filters (identical to that used for the H-∞ control laws) were again added to reject biases and low-frequency disturbances. The addition of the first-order washout filters further increased the controller order by two. These control laws were also too large to fit within the digital controller. As a result, internally balanced controller order reduction[13] was once again employed to reduce the order. The level of reduction that could be achieved was much less for these controllers than for the H-∞ controllers because of the more complex filter structure. The final order for control laws μ #1, μ #2, and μ #3 was 22, 26, and 24, respectively. Figures 9–11 present the frequency responses of the three reduced-order μ-synthesis control laws that were tested in the wind tunnel.

IV. Analysis and Experimental Results
A. Analysis

Each of the control designs just presented was able to achieve the design objectives to varying degrees. In this section the degree to which each of the control law designs accomplished the design objectives will be discussed. All of the analyses presented here were obtained using the P-Δ model in Fig. 5 and the mathematical model of the BACT system presented in Ref. 8.
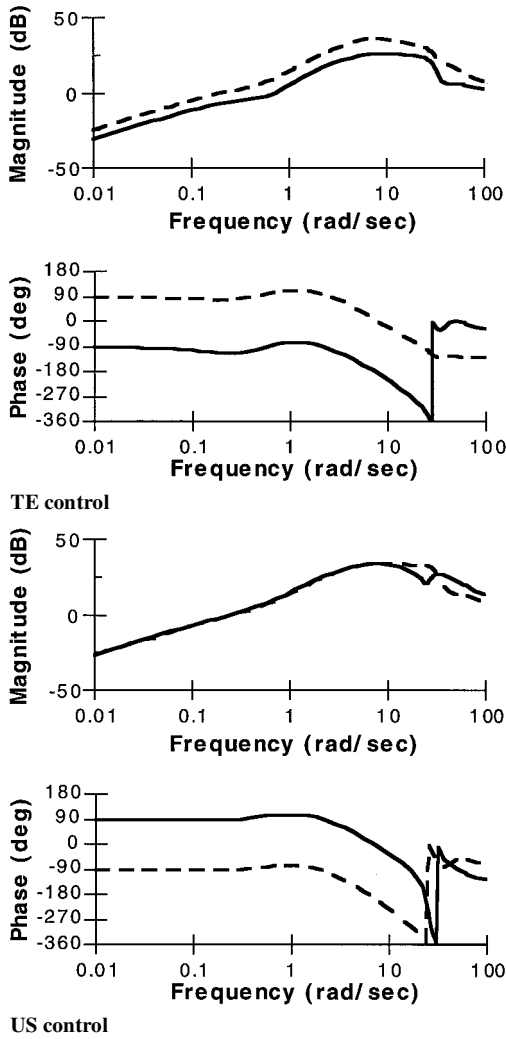
TE control

US control

Fig. 8 H-∞ #2 frequency response: ——, TEI accelerometer, and - - - -, LEI accelerometer.

Table 1   Predicted robustness properties of MIMO controllers ($M = 0.77, q = 175$ psf)

		SSVs	
Control law	Controller order	Stability robustness	Performance robustness
TE	3	4.3	6.5
US	3	4.2	4.6
TE+US	6	5.8	6.2
H-∞ #1	7	1.4	1.5
H-∞ #2	12	1.3	1.4
μ #1	22	2.4	4.2
μ #2	26	1.6	2.0
μ #3	24	4.6	5.3

TE control

US control

Fig. 9 θ #1 frequency response: ——, TEI accelerometer, and - - - -, LEI accelerometer.

The SISO control law designs were predicted to have excellent analytical stability margins over the entire range of operating conditions, but the margins for the trailing-edge flap control law were generally better than for the upper spoiler control law. Similarly, the MIMO control laws had excellent predicted stability margins (as indicated by the fact that each design had structured singular values near unity). However, the process of adding washout filters and reducing the controller order affected the robustness of the MIMO control laws by reducing the stability margins relative to the full-order designs.

Structured singular values (SSVs), based on the simple performance and control weights, are used as a basis for stability robustness comparisons among the various controllers. The uncertainty model is the constant unit-ball uncertainty used to perform the H-∞ and μ-synthesis designs. Table 1 summarizes the structured singular values for the various SISO and MIMO control laws.

Notice that none of the control laws had SSVs below one, which would guarantee stability subject to arbitrary uncertainties bounded in magnitude by the uncertainty weight. In fact, although the μ-synthesis controllers were initially designed to have SSVs of approximately one for unit uncertainty, the process of adding washout filters and reducing the controller order increased the SSVs to values above those for the H-∞ designs. However, the robustness was better than that achieved by either the trailing edge (TE) and upper spoiler (US) designs or their combination (TE + US). The μ-synthesis control law based on the more complex performance and control weights (i.e., μ #3) demonstrated the worst robustness of the MIMO designs. This controller also incurred the most reduction error during the controller reduction process.

SSVs can also provide a measure of performance robustness. Using the same weights and uncertainty model, the MIMO control laws were assessed for their ability to keep peak acceleration levels below 0.1 g and peak control deflections below 1.0 deg. An SSV of unity indicates that the performance objective is met by all systems bounded by the unit-ball uncertainty model. Table 1 summarizes the SSVs associated with performance robustness. Because the performance measure is very closely related to the stability measure, the performance results parallel the stability results. The SSVs indicate that, though the specific performance objective was not met, the MIMO designs were clearly superior to the SISO designs and successfully reduced acceleration levels with acceptable control activity.

Simulation studies of both the SISO and MIMO control laws were also conducted. Each of the control laws maintained stability over the entire range of simulated wind-tunnel operating conditions
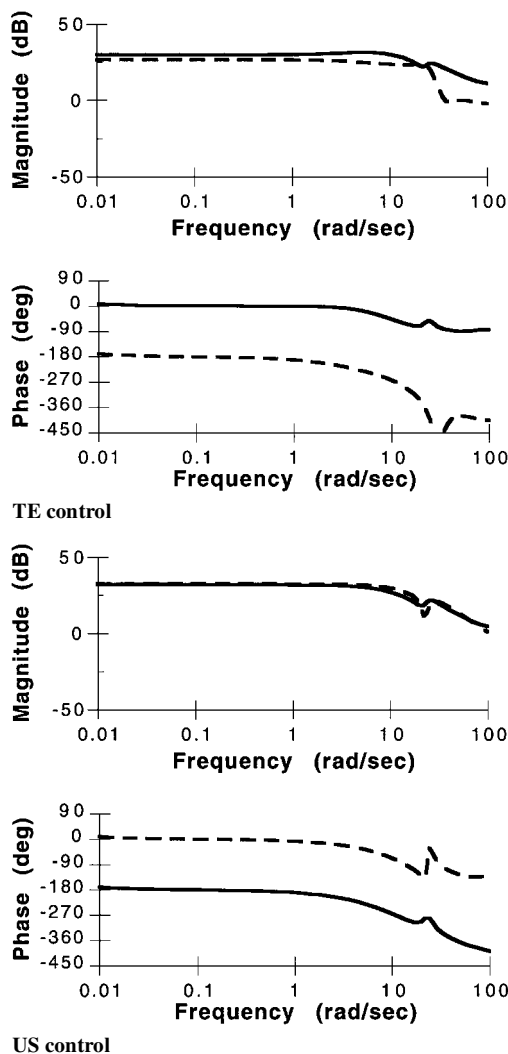
TE control

US control

Fig. 10 θ **#2 frequency response:** ———, **TEI accelerometer, and ----,**
LEI accelerometer.

—$M = 0.77$, $0 < q < 225$ psf. The performance levels of all of the control laws were very similar with rms accelerations on the order of 0.03 g. In addition, the MIMO designs were generally able to suppress large initial condition perturbations more effectively (i.e., exhibited shorter settling times).

One other design objective was to keep the controller order as small as possible in order to simplify the implementation and ensure that the limits of the digital controller were not exceeded. This proved to be a difficult task for the MIMO designs. Order reduction was required for these controllers to fit in the digital controller (Table 1). As a result, some of the robustness benefits of the μ-synthesis approach have been lost as is evident by the larger than unity SSVs for the reduced-order controls laws evaluated with the unit-ball uncertainty. This is most apparent for controller μ #3.

B. Experimental Results

The control laws were implemented in the BACT's digital control computer and used to control the BACT system over the entire range of wind-tunnel conditions: $0.5 < M < 0.95$ and $100 < q < 200$ psf. These conditions represent both open-loop stable and open-loop unstable conditions. All of the control laws were successful in suppressing flutter and maintaining closed-loop stability when the system was open-loop stable. In addition, the acceleration levels associated with the various controllers were quite acceptable with the MIMO designs somewhat better than the SISO designs. Table 2 summarizes the performance of the various control laws in terms of rms accelerations and control surface activity for an open-loop unstable condition.

Table 2   Experimental rms performance data for BACT
control laws ($M = 0.77$, $q = 175$ psf)

Control law	TEI acceleration, g	LEI acceleration, g	TE command, deg	US command, deg
TE	0.033	0.042	0.35	——
US	0.038	0.045	——	0.55
TE + US	0.029	0.038	0.22	0.44
H-∞ #1	0.03	0.03	0.31	0.34
H-∞ #2	0.03	0.03	0.32	0.29
μ #1	0.03	0.03	0.2	0.28
μ #2	0.03	0.03	0.25	0.17
μ #3	0.04	0.04	0.25	0.23

TE control

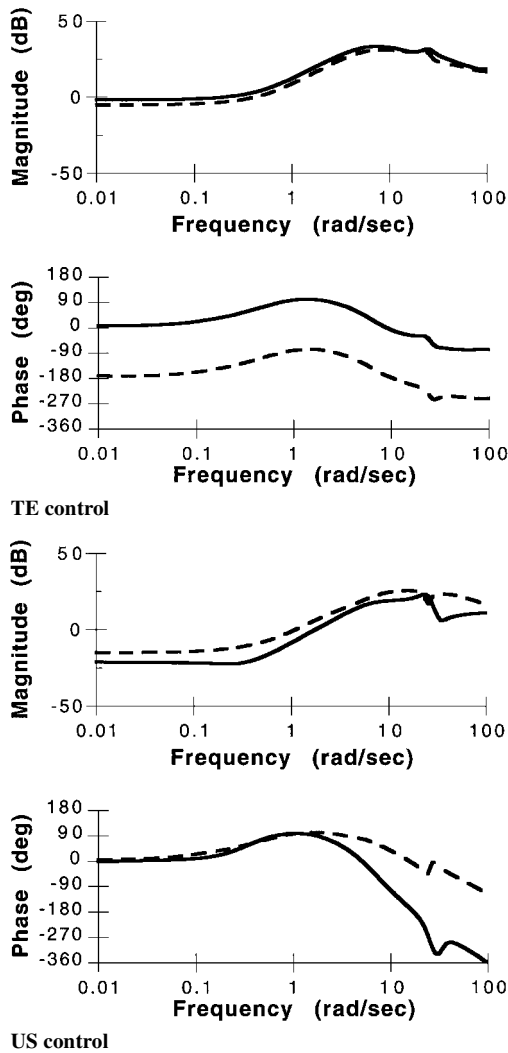
US control

Fig. 11 θ **#3 frequency response:** ———, **TEI accelerometer, and ----,**
LEI accelerometer.

The basic difference between the various controllers was the control activity required. This was not particularly evident during normal operations because all of the controllers required much less than 1.0-deg rms control inputs. However, when large oscillations were allowed to develop by disengaging the controller at an open-loop unstable condition, the control activity and system response that resulted when reengaging the controller was significantly lower for the MIMO designs. This can attributed to both the added control power associated with multiple control surfaces and the fully coupled nature of the MIMO control laws as demonstrated by the superiority of the MIMO control laws compared to the combination of the two SISO control laws.

Robustness was assessed experimentally using the CPE tool[3] to compute generalized robustness measures from response data.

Table 3 Experimental robustness data for BACT control laws (M = 0.76–0.79, q = 174–180 psf)

Control law	Min SV @ Input	Min SV @ Output
TE	0.84	0.45
US	0.36	0.08
TE + US	0.42	0.24
H-∞ #1	0.34	0.32
H-∞ #2	0.43	0.24
μ #1	0.6	0.67
μ #2	0.55	0.68
μ #3	0.4	0.29

Table 3 summarizes the robustness of the various control laws obtained from the CPE results in terms of the minimum singular values of the return difference matrix at the plant input and output. The μ-synthesis control laws have generally better robustness than the others.

V. Conclusions

The H-∞ and μ-synthesis robust multivariable control design methods have been successfully applied to the problem of wing flutter suppression for a simple wind-tunnel model. These methods have been shown to result in control laws that have similar nominal performance and better stability and performance robustness than more traditional SISO designs. In addition, a constant control law was able to maintain closed-loop stability over a very wide range of (open-loop stable and unstable) wind-tunnel operating conditions.

However, some of the benefits associated with robust multivariable control design were not fully realized. Controller reduction was required to fit the control laws into the control computer, and washout filters had to be added a posteriori to reject sensor biases. In addition, attempts to use uncertainty representations based on actual plant differences caused by dynamic pressure variations were unsuccessful for both the H-∞ and μ-synthesis designs. Each of these practical implementation issues reduced the performance and robustness of the resulting multivariable control law designs.

Besides the demonstration of robust multivariable control for flutter suppression, the BACT project has had several other valuable outcomes. Spoilers have been demonstrated to be an excellent option for applications to active flutter suppression. The BACT wind-tunnel model system has proven to be a very reliable active control testbed and offers excellent opportunities for future research. The mathematical model of the BACT system used for control system design has been extensively documented and is available for academic and research applications. The extensive database that has been collected is available to further develop aeroelastic modeling methods and control system design methods.

References

[1]Durham, M. H., Keller, D. F., Bennett, R. M., and Wieseman, C. D., "A Status Report on a Model for Benchmark Active Controls Testing," AIAA Paper 91-1011, April 1991.

[2]Bennett, R. M., Eckstrom, C. V., Rivera, J. A., Jr., Dansberry, B. E., Moses, G. F., and Durham, M. H., "The Benchmark Aeroelastic Models Program—Description and Highlights of Initial Results," NASA TM-104180, Dec. 1991.

[3]Wieseman, C. D., Hoadley, S. T., and McGraw, S. M., "On-Line Analysis Capabilities Developed to Support Active Flexible Wing Wind-Tunnel Model," *Journal of Aircraft*, Vol. 32, No. 1, 1995, pp. 39–44.

[4]Waszak, M. R., and Srinathkumar, S., "Flutter Suppression for the Active Flexible Wing: A Classical Design," *Journal of Aircraft*, Vol. 32, No. 1, 1995, pp. 61–67.

[5]Rivera, J. A., Jr., Dansberry, B. E., Durham, M. H., Bennett, R. M., and Silva, W. A., "Pressure Measurements on a Rectangular Wing with a NACA 0012 Airfoil During Conventional Flutter," NASA TM-104211, July 1992.

[6]"The Langley Transonic Dynamics Tunnel," Langley Working Paper, LWP-799, Hampton, VA, Sept. 1969.

[7]Scott, R. C., Hoadley, S. T., Wieseman, C. D., and Durham, M. H., "Benchmark Active Controls Technology Model Aerodynamic Data," *Journal of Guidance, Control, and Dynamics*, Vol. 23, No. 5, 2000, pp. 914–921.

[8]Waszak, M. R., "Modeling the Benchmark Active Control Technology Wind-Tunnel Model for Application to Flutter Suppression," AIAA Paper 96-3437, July 1996.

[9]Mukhopadhyay, V., "Transonic Flutter Suppression Control Law Design and Wind-Tunnel Test Results," *Journal of Guidance, Control, and Dynamics*, Vol. 23, No. 5, 2000, pp. 930–937.

[10]Balas, G. J., Doyle, J. C., Glover, K., Packard, A., and Smith, R., *μ-Analysis and Synthesis Toolbox (for Use with MATLAB)—User's Guide*, The MathWorks, Inc., and MUSYN, Inc., Natick, MA, July 1993.

[11]Doyle, J. C., and Stein, G., "Multivariable Feedback Design: Concepts for a Classical/Modern Synthesis," *IEEE Transactions on Automatic Control*, Vol. AC-26, No. 1, 1981, pp. 4–16.

[12]Anderson, M. R., "Linear Design Models for Robust Control Synthesis," *AIAA Guidance, Navigation, and Controls Conference*, AIAA, Washington, DC, 1989, pp. 263–270.

[13]Bacon, B. J., and Schmidt, D. K., "Multivariable Frequency-Weighted Order Reduction," *Journal of Guidance, Control, and Dynamics*, Vol. 12, No. 1, 1989, pp. 97–107.